IOSR Journal of Mechanical and Civil Engineering (IOSR-JMCE)
e-ISSN: 2278-1684,p-ISSN: 2320-334X, Volume 19, Issue 1 Ser. II (Jan. – Feb. 2022), PP 49-62
www.iosrjournals.org

Second Law Applied to a Straight Microchannel Printed Circuit Heat Exchanger using TiO_2 and Al_2O_3 as Nanoparticles

Élcio Nogueira[1], José Tomaz da Silva Teixeira[2]
Department of Mechanic and Energy, State University of Rio de Janeiro, Brazil
Adjunct Professor[1]; Engineer, graduate student at UNIFOA[2]

Abstract
Efficiency, effectiveness, and irreversibility concepts based on the second law of thermodynamics are applied to analyze the thermal performance of a Straight Microchannel Printed Circuit Heat Exchanger (PCHE). The microchannel is considered a basic counter-flow heat exchanger, where the water flows through the hot channel, and the nanofluid flows through the cold channel. In addition to the efficiency, effectiveness, and irreversibility parameters, the heat transfer rate and the outlet temperatures for both fluids were determined, with variations in the mass flow rate of both fluids. The thermal performance of the compact heat exchanger (PCHE) improves when nanoparticle fractions are included. Aluminum oxide nanoparticles Al_2O_3 have better thermal performance than titanium oxide nanoparticles TiO_2.

***Keywords**: Straight Microchannel; Printed Circuit Heat Exchanger; Nanofluid; Efficiency; Effectiveness.*

Date of Submission: 08-01-2022 Date of Acceptance: 22-01-2022

I. Introduction

The data and information used for theoretical analysis of a straight micro-channel Printed Circuit Heat Exchanger (PCHE) were taken from experimental and theoretical work, where thermal and dynamic performance tests were performed.

Efficiency, effectiveness, and irreversibility concepts based on the second law of thermodynamics are applied to determine analytically the thermal performance of a Straight Microchannel Printed Circuit Heat Exchanger (PCHE). The analysis carried out in this work includes nanoparticles of aluminum oxide Al_2O_3 and titanium oxide TiO_2 flowing in the cold channel of the PCHE.

The Printed Circuit Heat Exchanger (PCHE) has been used as alternatives to shell and tube heat exchangers. The name derives from the flat metal plates that form the core of the micro-channel. The plates through which the fluids pass are stacked, diffusion bonded, and become a solid metal block, usually stainless steel. Some of the advantages of PCHE are: optimized for counter-flow; compact, that is, high heat exchange surface area per unit volume; reduced space and structure; reduction in energy cost; smaller and lighter than conventional compact heat exchangers; high heat transfer coefficients. Disadvantages of PCHE: expensive; fluid extremely clean; blockages can occur but can be avoided with additional cost; need to be cleaned regularly; require chemical cleaning; insulation kit may be required Bahman Zohuri [1].

Zafar Said and Rahman Saidur [2] determined the thermophysical properties of TiO_2 and Al_2O_3 experimentally. Experiments were conducted to determine the viscosity and density range from 25 °C to 80 °C. An increase in the volume fraction increases the density and viscosity of the nanofluid. It was observed that the heat transfer coefficient increases with increasing mass flow rate and with the volume fraction of the nanofluid. Empirical formulas for density and viscosity were determined as a function of the volume fraction of the nanoparticles.

Figures 1 and 2, below, were taken from the experimental and theoretical work elaborated by Jang-Won Seo et al. [3]; what is the primary reference of this work, where thermal and dynamic performance tests were performed for a PCHE. Tests were performed for Reynolds numbers in the range of 100–850, with inlet temperatures equal to 50º and 20º. It was observed that the average heat transfer rate increased with increasing Reynolds number. Furthermore, empirical correlations for the heat transfer coefficient as a function of the Reynolds number were developed. The authors state that PCHE has applications in various fields such as fuel cell systems, refrigeration, air conditioning systems, etc.

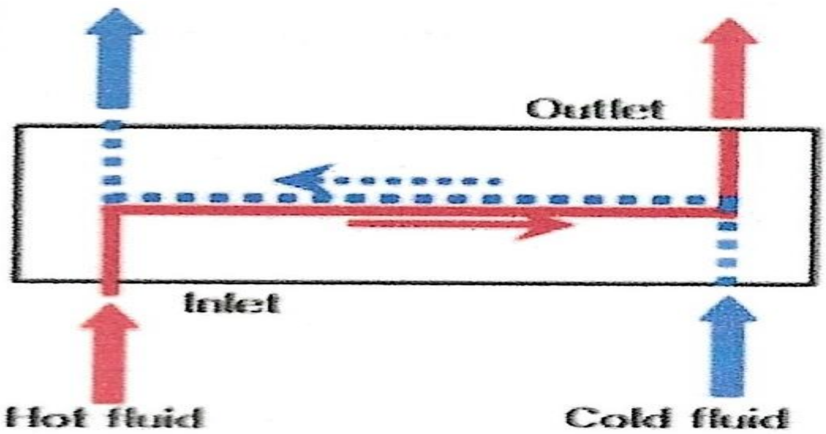

Figure 1 – Schematic representation of a counter-flow heat exchanger for microchannel Printed circuit heat exchanger (PCHE) (Reference [3]).

Figure 2 – Final shape of a microchannel heat exchanger (PCHE) (Reference [3]).

Emanuele Zanetti et al. [4] argue that minimization of the refrigerant charge and the use of new refrigerants can be essential factors for the development of new technologies related to heat exchangers and that micro-channel technology is one of the options. They feature a microchannel heat exchanger working both as a condenser and an evaporator, develop a microchannel heat exchanger model, and compare the performance with experimental measurements. The results obtained through the model were compared with a traditional finned coil heat exchanger. It has been demonstrated that the charge contained within the tubes can be reduced by about 30% using the micro-channel heat exchanger.

Salah Almurtaji et al. [5] provide a systematic review of the state-of-the-art heat exchanger technology using nanofluids for enhancing their thermal-hydraulic performance. The work aims to emphasize the vital role of nanofluids and how these advanced fluids can significantly increase the thermal efficiency of heat exchangers. The review shows that using nanofluids results in a higher heat transfer enhancement.

Yanhui Han et al. [6] analyze the advantages and disadvantages of using micro-channel heat exchangers. States that micro-channel heat exchangers can reduce equipment weight, lower manufacturing costs, and improve product competitiveness by using new materials such as nanofluids. They have been widely applied in electronic equipment cooling and gradually in automotive air conditioning systems. Besides these, the micro-channel heat exchanger is very different in the flow and heat transfer characteristics, and that these differences can be attributed to scaling effects. Furthermore, they claim that traditional thermal performance can be improved by adequately exploiting micro-channel geometry and size, as they are essential to heat exchanger design. Finally, they believe that micro-channel type heat exchangers will be more widely used when existing problems in manufacturing and applications are resolved.

Harish Kumar Patel et al. [7] deals with nanofluid's importance, application, and challenges in microchannel heat exchangers. Theoretical model and empirical equation for thermal conductivity were proposed to determine the thermal performance associated with the nanofluid. Furthermore, the application of nanofluids in microchannels was analyzed using different geometric configurations under various boundary conditions. They concluded that more investigation is required about the effects of other nanoparticles, fractional volume, and particle size on the micro-channel heat exchanger performance.

Seungjoon Baik et al. [8] describe the result of the design, construction, and applicability to the S-CO2 cycle of a PCHE. They claim that the PCHE design needs to accurately predict the thermal performance and pressure drop for the S-CO2 Brayton cycle. Therefore, they developed an analysis and design code called KAIST_HXD, and used it to design and test accuracy on a small PCHE. The result of the experiment showed acceptable performance and also small pressure drops. In addition, the design code and experimental data determined high efficacy, above 90%, within a small 200 mm core.

Sushant S. Bhosale and Anil R. Acharya [9] claim that the world is moving towards miniaturization. To ensure high thermal performance associated with the long life of the equipment, highly compact systems are needed. Microchannels are natural candidates as they provide large heat transfer surface area per unit volume. Microchannels have great potential and can be used in numerous applications, such as rocket engines, refrigeration, microgravity thermal control, capillary pump circuits, and many others. Furthermore, using microchannel heat exchangers reduces the amount of refrigerant to be used, reducing operating costs.

The work developed by Lei Chai and Savvas A. Tassou [10] provides a comprehensive review for understanding the performance of PCHEs. They begin by presenting the fundamental theoretical principles of a PCHE, material selection, fabrication, and assembly techniques. Next, optimization of the design of PCHE is discussed, considering aspects related to heat transfer rate increase, pressure drop, compaction, fluid inventory, and capital cost. Finally, the analysis cites heat exchangers and projects under development. They claim that a lot of work is needed to increase the attractiveness of PDHEs to a wide range of applications and cite the need to select materials to improve thermal performance, to increase the operating capacity at high temperatures and pressure.

Ahmad Fakheri [11] defines thermal efficiency for heat exchangers based on the second law of thermodynamics. He demonstrates an ideal heat exchanger of the balanced counter-flow type. The ratios between the thermal capacities of the ideal heat exchanger are equal to the minimum thermal capacity ratio of an actual heat exchanger. As a result, the ideal heat exchanger generates minimal entropy, allows maximum heat exchange, and is less irreversible. Efficiency, defined as the ratio of the heat transfer rate of the heat exchanger to that of the ideal heat exchanger, provides a new way to design and analyze heat exchangers.

Roopesh Tiwari and Govind Maheshwari [12] determine the efficiency and effectiveness of counter-flow and parallel flow heat exchangers by applying the second law of thermodynamics. However, the performance of a heat exchanger is generally measured by its effectiveness, and this parameter does not provide information about efficiency and irreversibility. Therefore, they establish the relationship between effectiveness and efficiency based on thermal irreversibility, which measures the degree of entropy generation in a physical system.

Nogueira, E. [13] applies the second law of thermodynamics to obtain the exit temperatures of fluids in a shell and tube heat exchanger. Water flows in the shell, and a water-ethylene glycol mixture is associated with volume fractions of nanoparticles in the tube. Water enters the reservoir at 27 °C and mixes at 90 °C. The mass flow in the shell is kept fixed, equal to 0.23 kg/s. The volume fractions of Ag and Al_2O_3 nanoparticles are equal to 0.01, 0.10, and 0.25. Heat transfer rate, efficiency, effectiveness, and irreversibility are presented to discuss results. It is demonstrated that the flow regime has a significant effect on the thermal performance of the heat exchanger.

Nogueira, E [14] presents a case study in a shell and helical coil tube heat exchanger where the water is heated. Ammonium nitrate is added at a given mass flow rate. It determines the flow rate and the saturation temperature of the steam necessary for heating a solution of water and ammonium nitrate (ANSOL) without crystallization of the solution. It uses the concepts of efficiency and effectiveness to determine the heat transfer rate that satisfies the imposed conditions within a certain degree of safety and at the lowest possible cost in steam generation. The intermediate quantities needed to reach the objective are the Reynolds number, the Nusselt number, and the global heat transfer coefficient.

Methodology

Table 1 – Hot (Water), cold (Ethylene Glycol 50%) fluids and nanoparticles properties

	ρ kg/m^3	k W/ (m K)	Cp J/(kg K)	μ kg/(m s)	ν m/s^2	α m/s^2	Pr
Hot	**994**	**0.623**	**4178**	**$0.72\ 10^{-3}$**	**$7.24\ 10^{-7}$**	**$1.5\ 10^{-7}$**	**4.83**
Cold	**1067.5**	**0.3799**	**3300**	**$3.39\ 10^{-3}$**	**$2.4045\ 10^{-5}$**	**$1.08\ 10^{-7}$**	**0.02**
Al_2O_3	**3950**	**31.92**	**873.34**	**-**	-	**$9.25\ 10^{-6}$**	**-**
TiO_2	**4250**	**8.95**	**686**	**-**	-	**$3.07\ 10^{-6}$**	**-**

Table 1, above, gives the properties of hot, cold fluids and nanoparticles of Al_2O_3 and TiO_2.
The Einstein equation calculates the viscosity of the nanoparticles:

$$\mu_{Particle} = \mu_C(1 + 2.5\,\phi) \qquad \mathbf{1}$$

$$Dh_C = \frac{4\, Ac_C\, Lf_C}{As_C} \tag{2}$$

Dh_C is the hydraulic diameter, $Ac_C = 42.2\ 10^{-6}$ m^2 $Lf_C = 137\ 10^{-3}$ m, $Lf_C = 137\ 10^{-3}$ m is the length of the cold flow stream, $Asc = 34.716\ 10^{-3}$ m^2 is the total cold area of the heat transfer area.

$$Dh_h = Dh_C \tag{3}$$

$$Lf_h = \frac{Dh_h\, As_h}{4\, Ac_h} \tag{4}$$

Lf_h is the length of the hot flow stream, $As_h = 26.037\ 10^{-3}$ m^2 is the total hot area of heat transfer area, Lf_h is the length of the hot flow stream.

The properties of the nanofluids are:

$$\rho_{nano} = \rho_{Particle}\,\phi + (1-\phi)\,\rho_C \tag{5}$$

$$\mu_{nano} = \frac{\mu_C}{(1-\phi)^{2.5}} \tag{6}$$

$$Cp_{nano} = \frac{Cp_{Particle}\,\rho_{Particle}\,\phi + (1-\phi)\,Cp_C\,\rho_C}{\rho_{nano}} \tag{7}$$

$$k_{nano} = \frac{[k_{Particle} + 2\,k_C + 2\,(k_{Particle} - k_C)\,(1-0.1)^3\,\phi]}{[k_{Particle} + 2\,k_C + 2\,(k_{Particle} - k_C)\,(1-0.1)^2\,\phi)}]\,K_c \tag{8}$$

$$\nu_{nano} = \frac{\mu_{nano}}{\rho_{nano}} \tag{9}$$

$$\alpha_{nano} = \frac{k_{nano}}{\rho_{nano}\,Cp_{nano}} \tag{10}$$

$$Pr_{nano} = \frac{\mu_{nano}}{\alpha_{nano}} \tag{11}$$

$$\mu_W = \frac{\mu_{nano} + \mu_h}{2} \tag{12}$$

μ_W is the assumed value for the fluid viscosity in the channel wall.

$$h_{nano} = 0.1706\ \ 6^{0.44}\,Re_{nano}{}^{0.324}\,Pr_{nano}{}^{\frac{1}{3}}\left(\frac{\mu_{nano}}{\mu_W}\right)^{0.14}\left(\frac{k_{nano}}{Dh_C}\right) \tag{13}$$

$$h_h = 0.1729\ 5^{0.44}\,Re_h{}^{0.324}\,Pr_h{}^{1/3}\left(\frac{\mu_h}{\mu_W}\right)^{0.14}\left(\frac{k_h}{Dh_h}\right) \tag{14}$$

The heat transfer coefficients of both fluids, cold (h_{nano}) and hot (h_h), were obtained by regression fit [3].

$$A_{Med} = \frac{As_h + As_C}{2} \tag{15}$$

The overall heat transfer coefficient is given by:

$$UoA = \frac{1}{\frac{1}{h_h\,As_h} + \frac{1}{h_{nano}\,As_c} + \frac{L}{k_{Metal}\,A_{Med}}} \tag{16}$$

$k_{Metal} = 16.2$ W/(m K) is the thermal conductivity of the heat transfer plate and $L = 0.4\ 10^{-3}$ m is the gap between the cold and hot channels.

$$\dot{m}_h = \frac{Re_h\,\mu_h\,Ac_h}{Dh_h} \tag{17}$$

$$\dot{m}_{nano} = \frac{Re_{nano}\,\mu_{nano}\,Ac_C}{Dh_C} \tag{18}$$

$\dot{m}_h$ and $\dot{m}_{nano}$ are the mass flow rates of the hot and cold fluid, respectively.

$$C_h = \dot{m}_h\,Cp_h \tag{19}$$

$$C_{nano} = \dot{m}_{nano}\,Cp_{nano} \tag{20}$$

C_h and C_{nano} are the heat capacity of the hot and cold fluid, respectively.

$$C^* = \frac{C_{min}}{C_{max}} \tag{21}$$

Were C_{min} is the minimum between C_h and C_{nano}.

$$NTU = \frac{UoA}{C_{min}} \tag{22}$$

NTU are the number of thermal units associated with the heat exchanger.

$$Fa = \frac{NTU\,(1-C^*)}{2} \tag{23}$$

Fa is the fin analogy for a counter-flow heat exchanger [11; 12].

$$\boldsymbol{\eta_T = \frac{tanh(Fa)}{Fa}} \qquad \mathbf{24}$$

$\boldsymbol{\eta_T}$ is the thermal efficiency.

$$\boldsymbol{\varepsilon_T = \frac{1}{\frac{1}{\eta_T\, NTU} + \frac{1 + C^*}{2}}} \qquad \mathbf{25}$$

$\boldsymbol{\varepsilon_T}$ is the thermal effectiveness.

$$\boldsymbol{\dot{Q}_{Max} = (Th_i - Tc_i)\, C_{min}} \qquad \mathbf{26}$$

$\boldsymbol{\dot{Q}_{Max}}$ is the maximum of the heat transfer rate for the situation in analysis.

$$\boldsymbol{\dot{Q} = \frac{(Th_i - Tc_i)\, C_{min}}{\frac{1}{\eta_T\, NTU} + \frac{1 + C^*}{2}}} \qquad \mathbf{27}$$

$\boldsymbol{\dot{Q}}$ is the actual heat transfer rate.

The outlet temperatures for both fluids, Th_O and Tc_O, are given by:

$$\boldsymbol{Th_O = Th_i - \frac{\dot{Q}}{\dot{m}\, Cp_h}} \qquad \mathbf{28}$$

$$\boldsymbol{Tc_O = Tc_i - \frac{\dot{Q}}{\dot{m}\, Cp_{nano}}} \qquad \mathbf{29}$$

$$\boldsymbol{\sigma_T = \left(\frac{C_h}{C_{min}}\right) ln\left(\frac{Th_o}{Tc_i}\right) + \left(\frac{C_{nano}}{C_{min}}\right) ln\left(\frac{Tc_o}{Tc_i}\right)} \qquad \mathbf{30}$$

$\boldsymbol{\sigma_T}$ is the thermal irreversibility for the heat exchanger.

II. Results And Discussion

Figure 3 presents the thermal efficiency of the heat exchange process between fluids with the Reynolds number in the cold fluid equal to the Reynolds number in the hot fluid, with nanofluid fractions as a parameter. Thermal efficiency is high for the entire analyzed flow range, approaching 100% for high Reynolds numbers. The flow rates are, in fact, the main factors for the observed high performance, and the nanoparticles did not present great relevance for the determination of the thermal efficiency within the analyzed volume fraction range.

Figure 4 shows how the influence of nanoparticles is significant and allows us to establish that larger fractions of nanoparticles show a slight decrease in thermal efficiency. Furthermore, the effect of aluminum oxide is more noticeable than titanium dioxide.

Figure 5 demonstrates that effectiveness decreases with increasing Reynolds number in both fluids and that larger nanoparticles have higher values for thermal effectiveness. However, thermal effectiveness is reasonably high for low Reynolds numbers and average for higher Reynolds numbers.

Thermal irreversibility shows the same trend as effectiveness, decreasing with the increase in the Reynolds number in both fluids and with higher values for more significant fractions in the volume of nanoparticles, as shown in Figure 6.

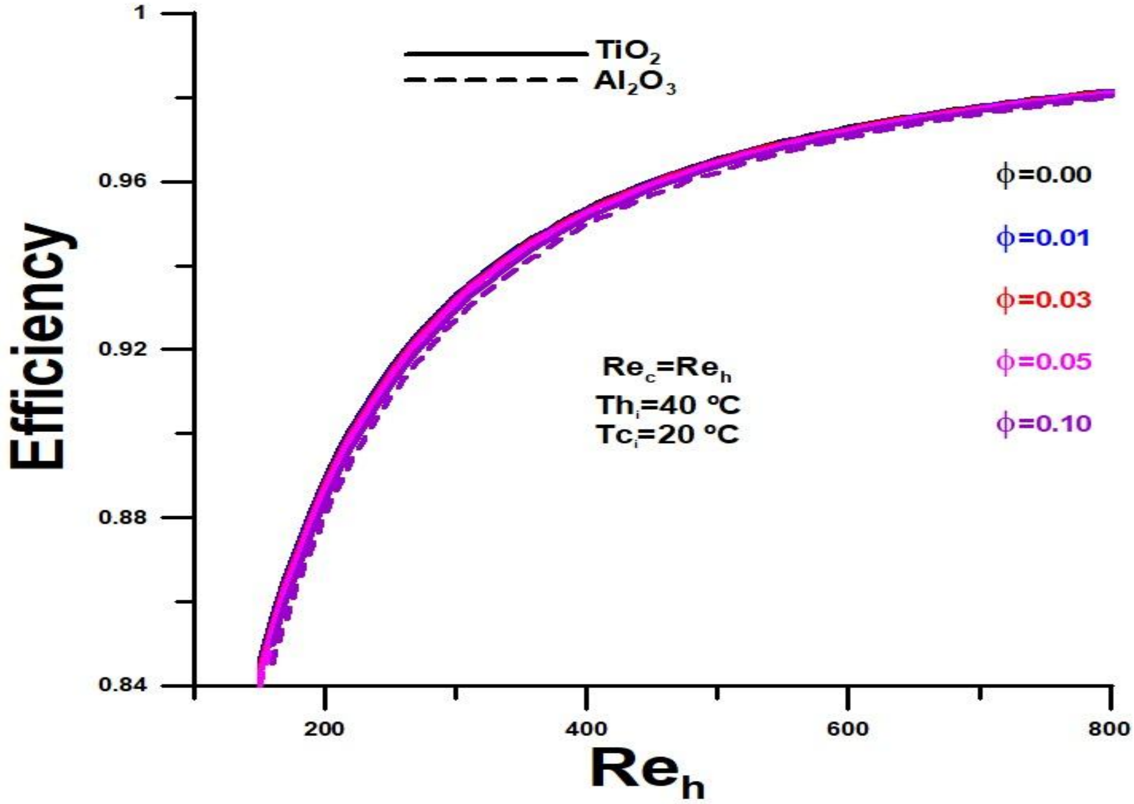

Figure 3 – Efficiency versus Reynolds number of the hot fluid with $Re_c = Re_h$

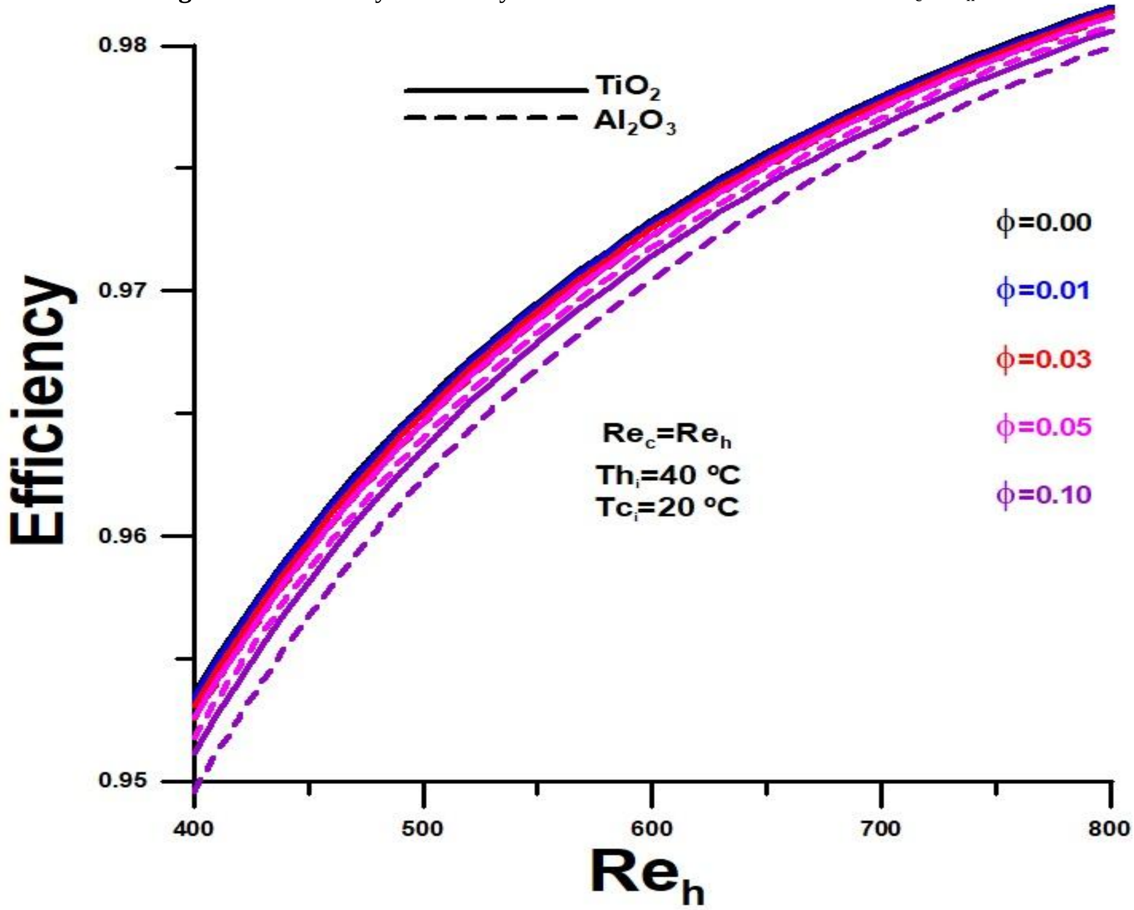

Figure 4 – Influence of the nanoparticles fraction at the Efficiency for $Re_c = Re_h$

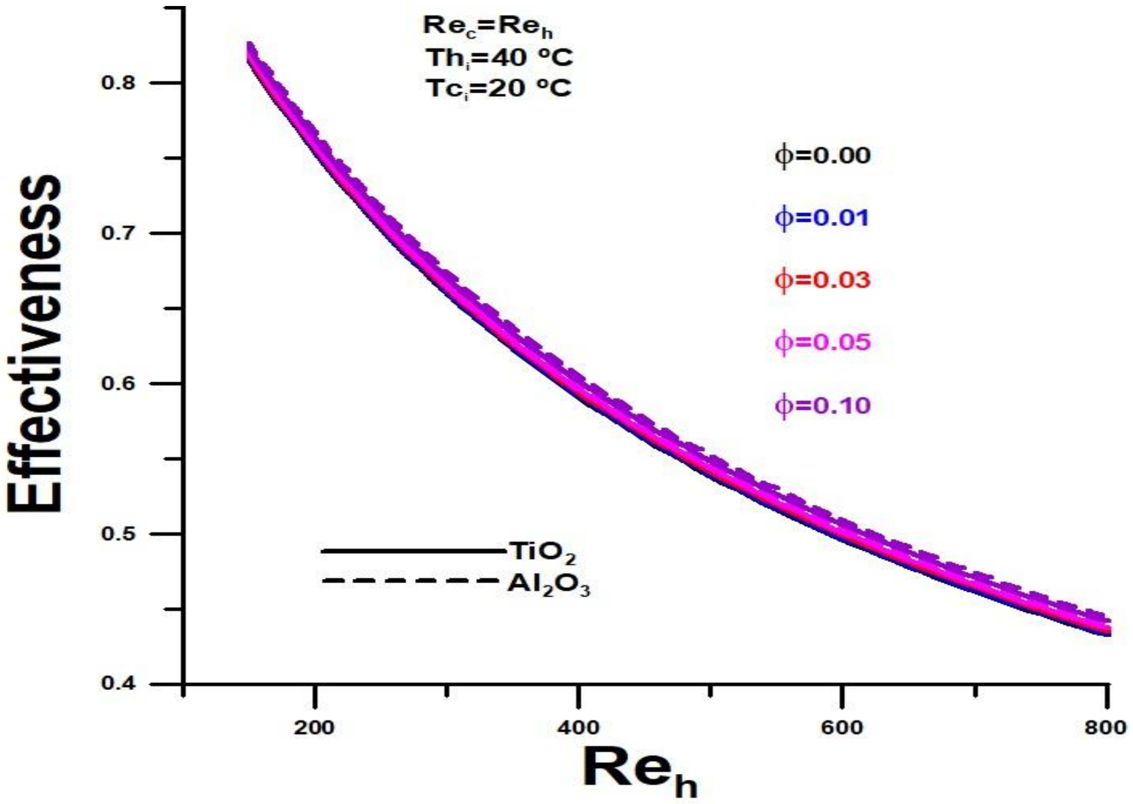

Figure 5 - Effectiveness versus Reynolds number of the hot fluid with $Re_c=Re_h$

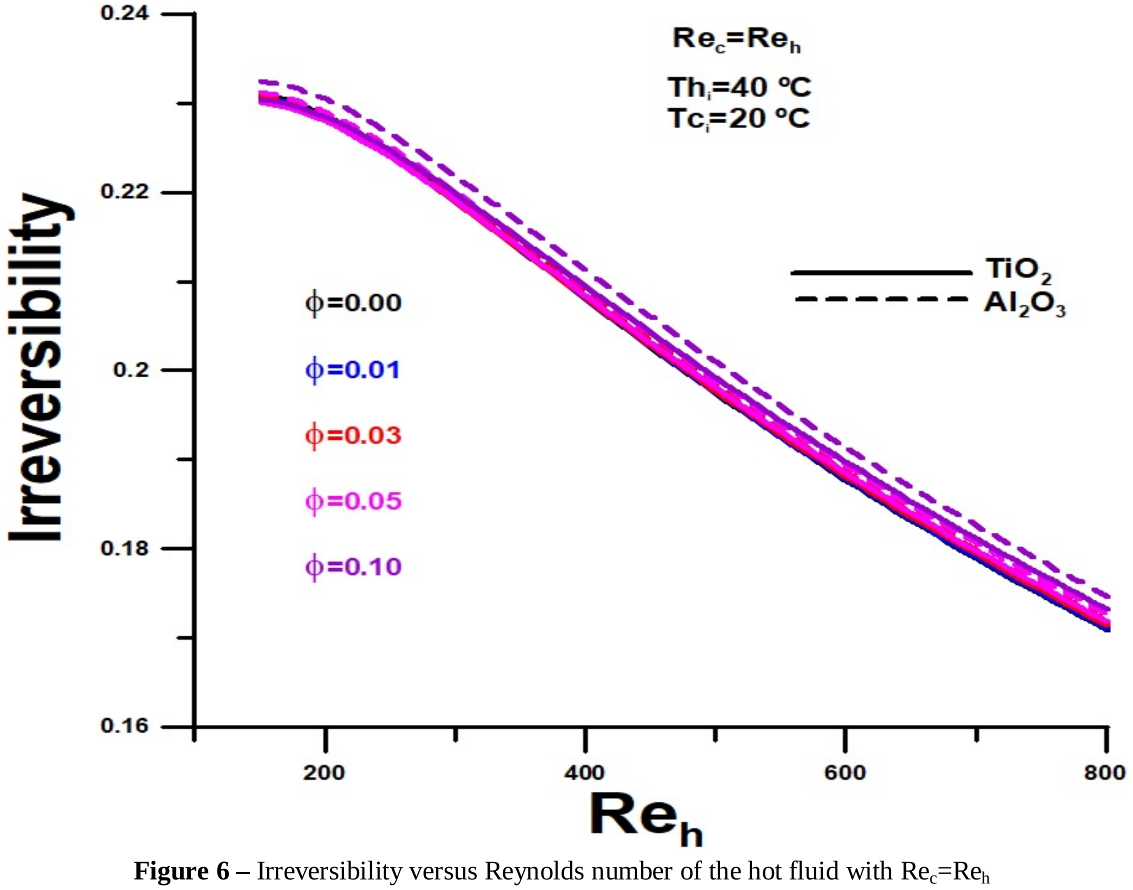

Figure 6 – Irreversibility versus Reynolds number of the hot fluid with $Re_c=Re_h$

The results presented in Figures 4, 5, and 6 show some relevant aspects about the heat exchange process between fluids. Thermal irreversibility measures the degree of entropy generation without considering viscous dissipation and, therefore, has low relative values. It is evident that entropy generation for smaller Reynolds numbers is superior to entropy generation for larger Reynolds numbers; there is more energy exchange in the form of heat exchange between fluids when the Reynolds number is low. Suppose there is more heat being generated and exchanged between the fluids. It means that the effectiveness must be greater, as it measures the fraction of heat exchanged between the fluids concerning the maximum theoretical exchange possible. Whenever there is greater heat exchange, that is, greater entropy generation, the lower the efficiency of the process must be. Higher volume fractions of nanoparticles enable greater irreversibility, with greater weight for aluminum oxide.

Figure 7 presents results for thermal efficiency as a function of the volume fraction of the nanoparticles for the highest Reynolds number of the nanofluid considered for analysis. The Reynolds number in the hot fluid is regarded as a parameter and varies between the lowest and highest values analyzed. As already observed in Figure 3, the efficiency is lower for smaller Reynolds numbers and great, close to 1, for more significant deals, with less influence on the volume fraction of the nanoparticles.

As expected, according to Figures 5 and 6, thermal effectiveness and thermal irreversibility have high values for lower values for the Reynolds number in both fluids, as shown in Figures 8 and 9. This result corresponds to higher heat transfer rates being exchanged between fluids.

Figure 10 presents actual heat transfer rates compared to the maximum theoretical heat transfer possible. For smaller Reynolds numbers, the closest is the actual heat transfer rate from the maximum possible heat transfer rate, which is reflected for high values of effectiveness and irreversibility. It is evident that greater effectiveness does not mean greater heat transfer rate but that the current and maximum rate relationship is high. When the Reynolds numbers increase, the distance between the observed values for the actual heat transfer rate and the maximum heat transfer rate is further apart, implying lower values for effectiveness and irreversibility. Despite this significant difference between the current and maximum values for the heat transfer rate, for high Reynolds numbers, Figure 3 demonstrates that the thermal efficiency is close to 1 and that the possibility of increasing the heat transfer rate between the fluids, which has a defined physical limit, decrease.

As Figuras 11 e 12 corroboram a conclusão acima, mostrando que quando o número de Reynolds do nanofluido aumenta, a diferença entre as taxas de transferência de calor local diminui, tendendo para zero. Um aumento no número de Reynolds do fluido frio, a partir de um determinado valor, não traz consequências significativas na variação da taxa de transferência de calor. No entanto, para alto número de Reynolds no fluido quente, aumenta a possibilidade de aumentar o número de Reynolds no fluido frio. A taxa máxima de transferência de calor aumenta com o número de Reynolds do fluido quente, pois tem a menor capacidade térmica, conforme mostrado na Figura 13.

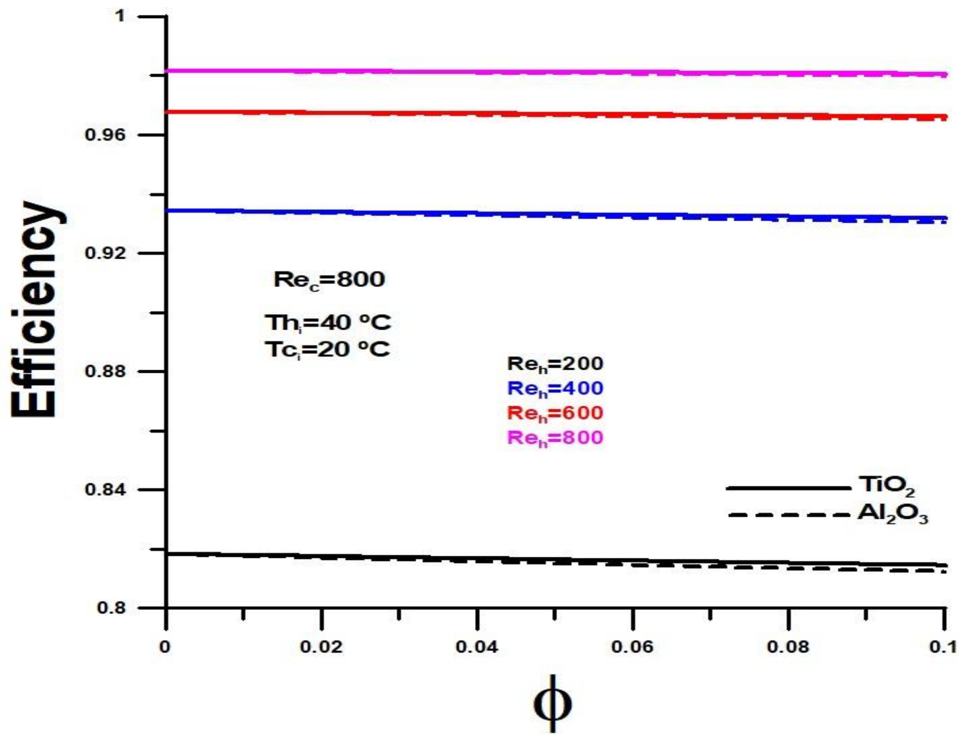

Figure 7 – Efficiency versus nanoparticles fractions with Re_c=800 and Re_h varying

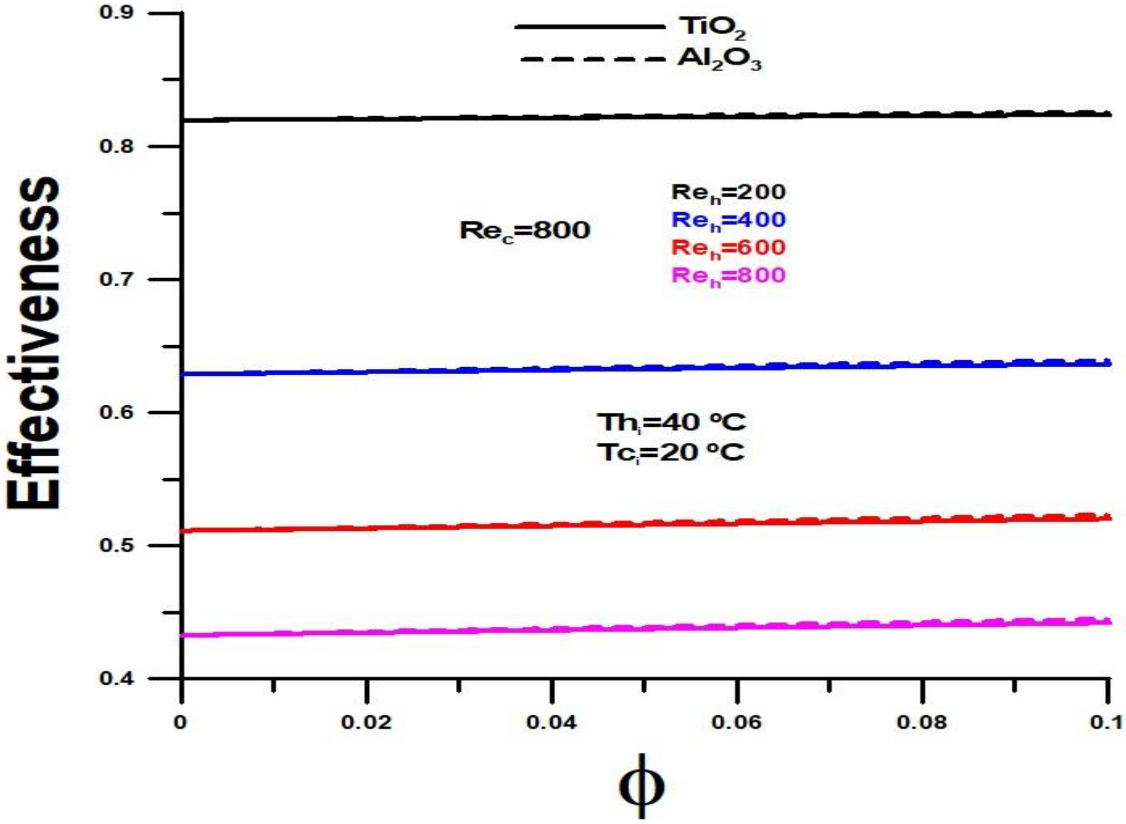

Figure 8 – Effectiveness versus nanoparticles fractions with Re_c=800 and Re_h varying

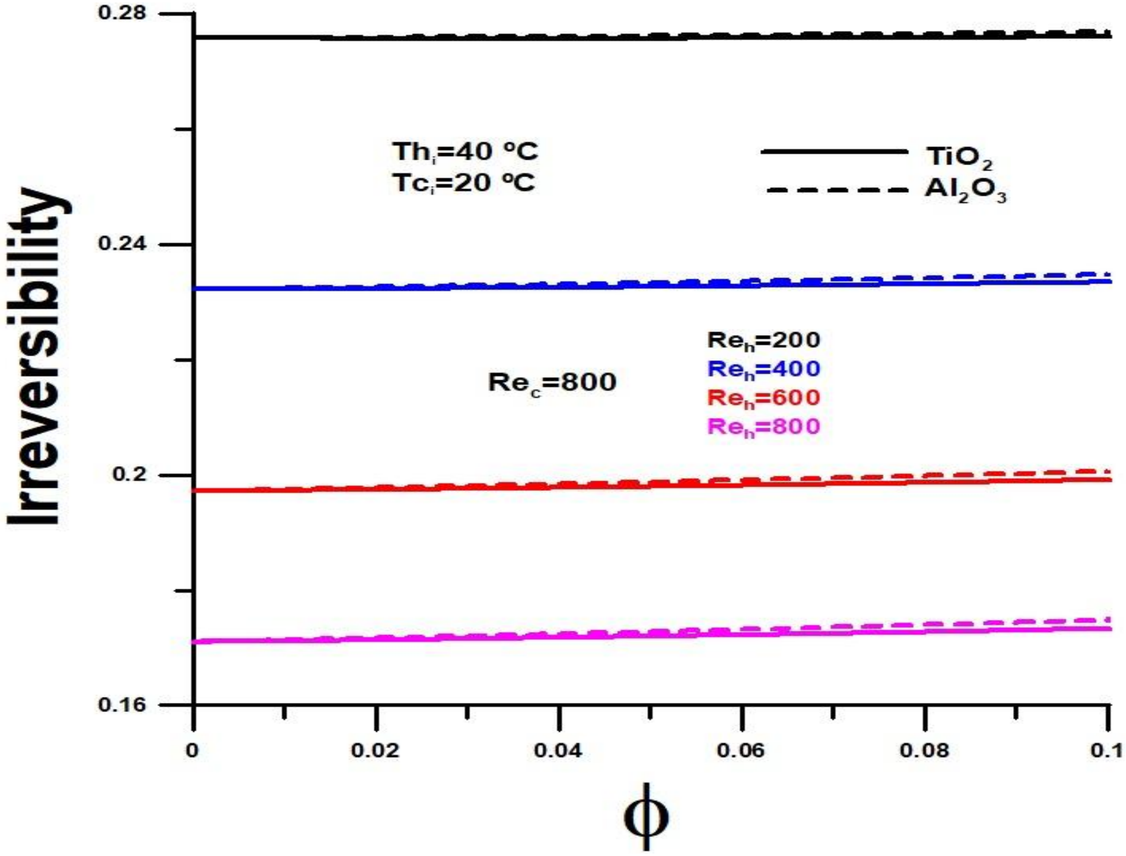

Figure 9 – Irreversibility versus nanoparticles fractions with Re_c=800 and Re_h varying

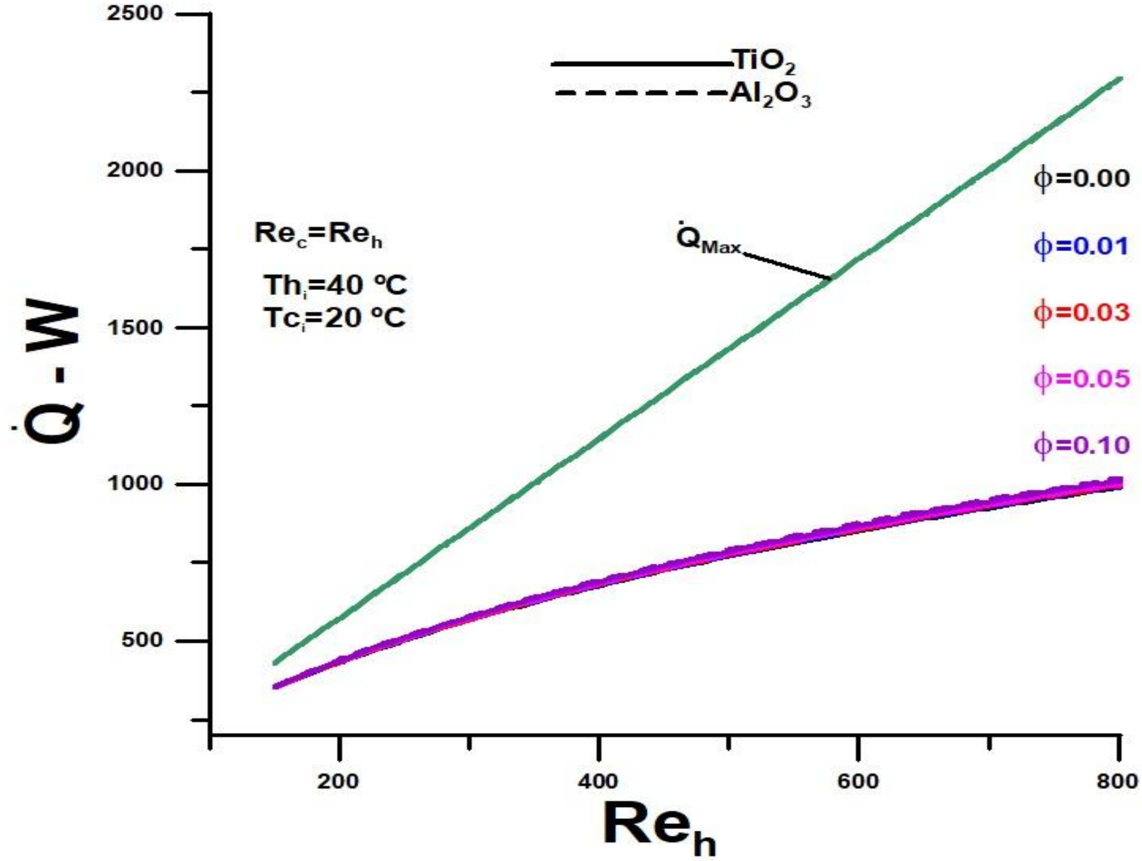

Figure 10 – Influence of the nanoparticles fraction at the heat transfer rate for Re_c=Re_h

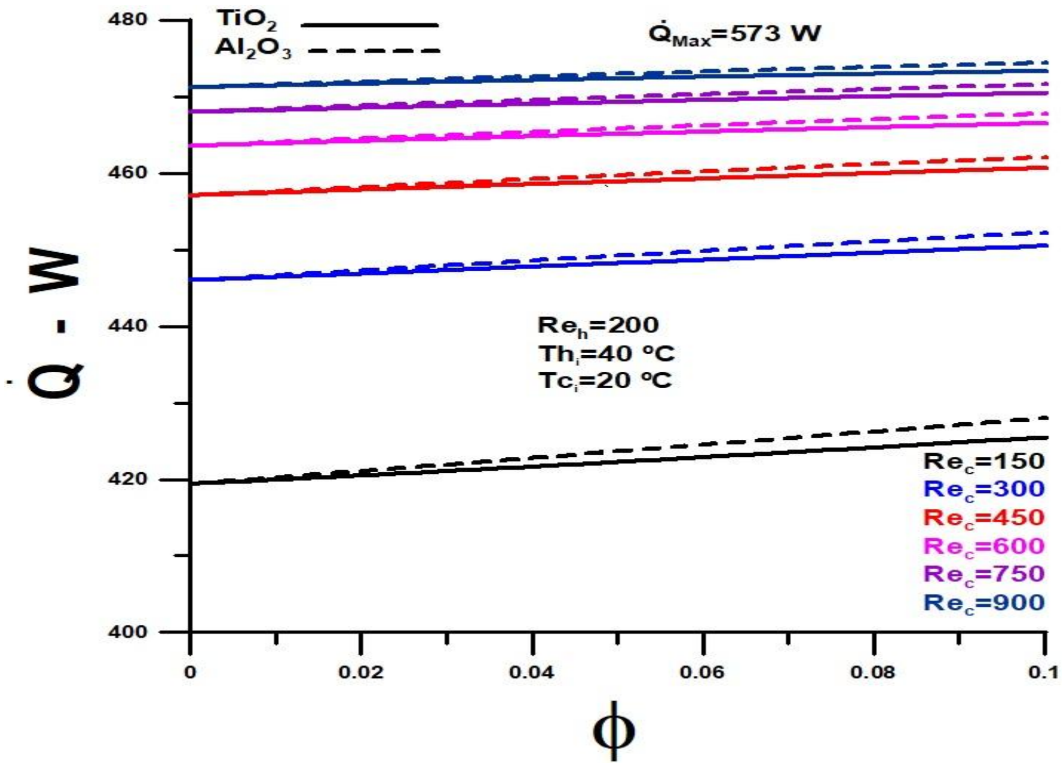

Figure 11 – Heat transfer rate versus nanoparticles fractions with Re_h=200 and Re_c varying

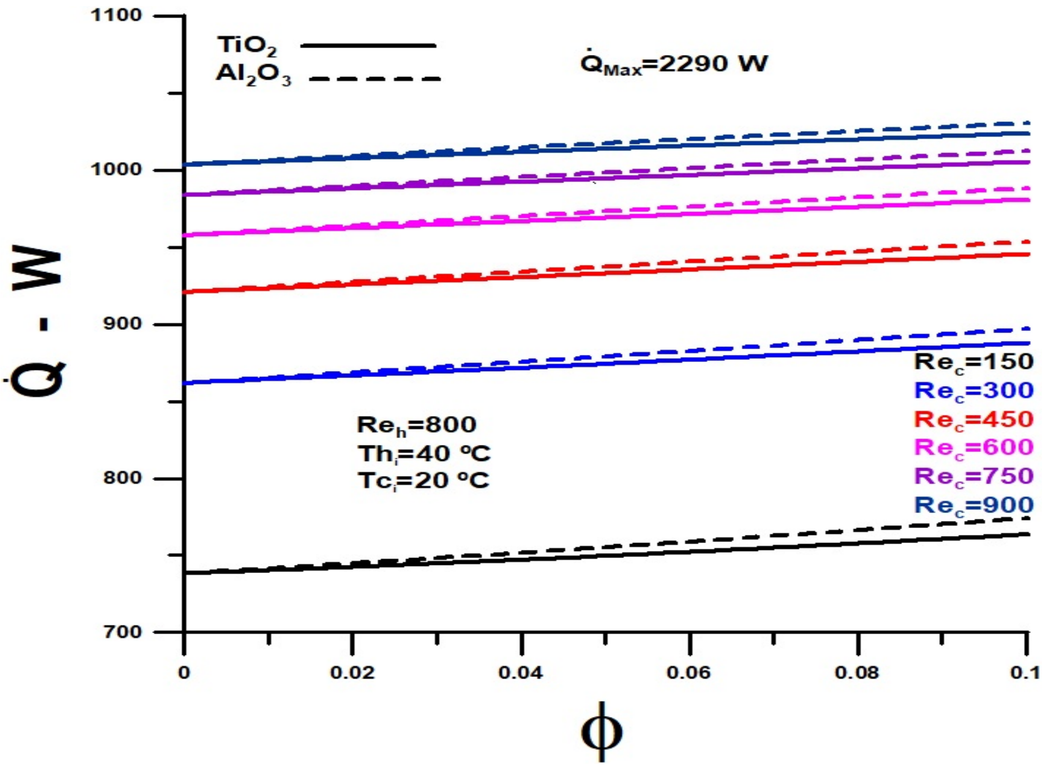

Figure 12 – Heat transfer rate versus nanoparticles fractions with Re_h=800 and Re_c varying

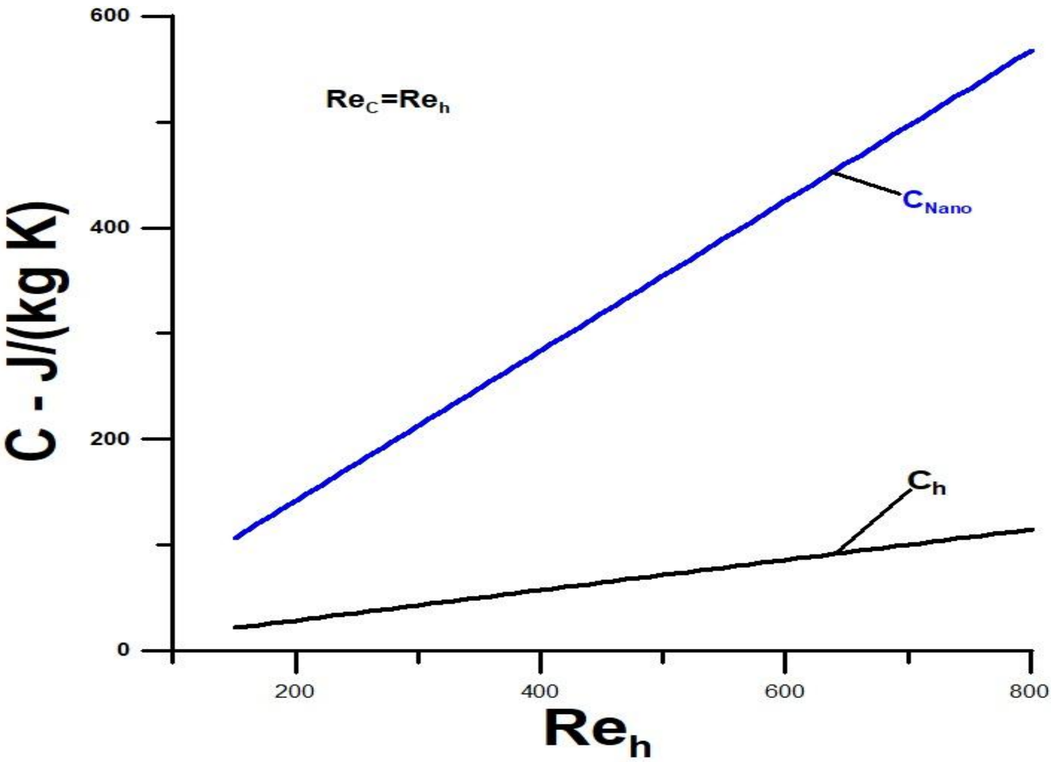

Figure 13 – Thermal capacity of the fluids versus Reynolds number of the hot fluid with Re_c=Re_h

When there is more significant entropy generation, greater irreversibility, and greater energy exchange between the fluids, the hot fluid outlet temperature is lower. Figure 14 presents the desirable fluid exit temperature values, which are smaller for a low Reynolds number value in both fluids. The influence of nanoparticles within the analyzed flow range is low.

The influence of nanoparticles on the hot fluid exit temperature is most conveniently represented in Figure 15, in the lower range of values for Reynolds numbers, with aluminum oxide demonstrating better thermal performance than titanium dioxide.

When there is more significant entropy generation, greater irreversibility, and greater energy exchange between the fluids, the cold fluid outlet temperature is greater. Figure 16 presents the cold fluid exit temperature values, more significant for the low Reynolds number value in both fluids. The influence of nanoparticles within the analyzed flow range is low.

The influence of nanoparticles on the exit temperature of the cold fluid is more conveniently represented in Figure 17, in the upper range of values for the Reynolds numbers, with aluminum oxide demonstrating better thermal performance than titanium dioxide.

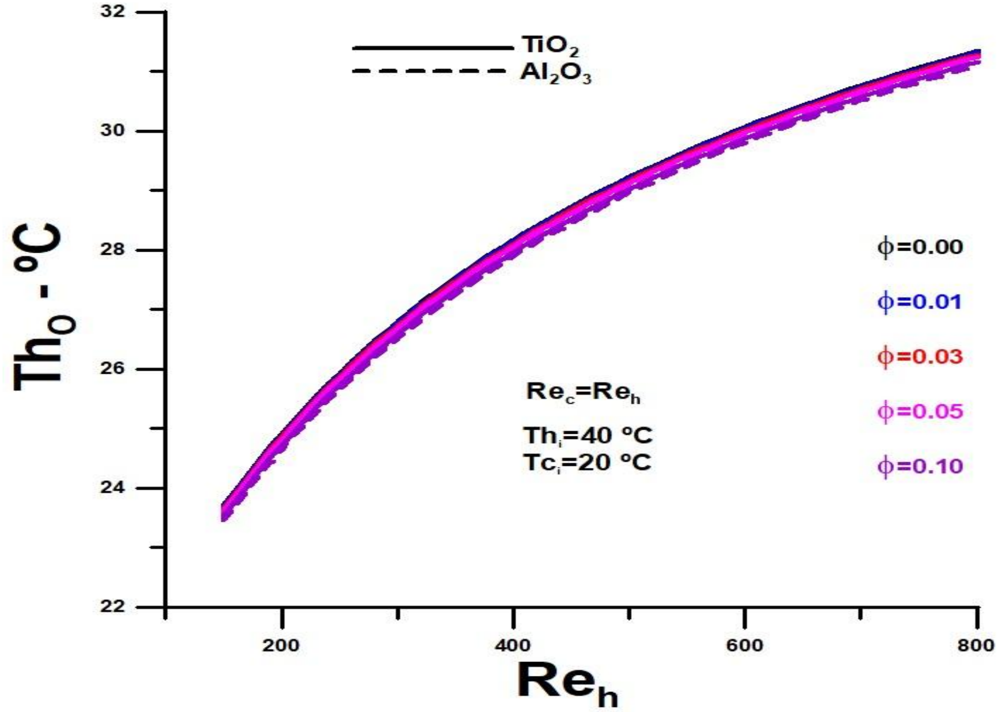

Figure 14 – Hot fluid temperature exit versus Reynolds number of the hot fluid with Re_c=Re_h

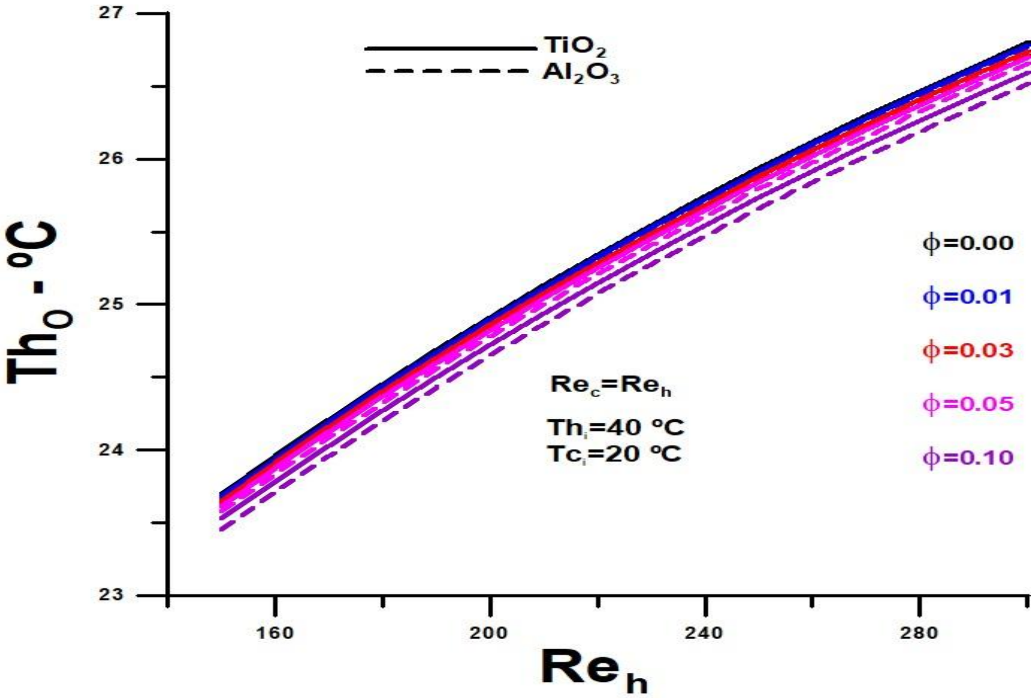

Figure 15 – Influence of the nanoparticles fraction at the hot fluid temperature exit for Re_c=Re_h

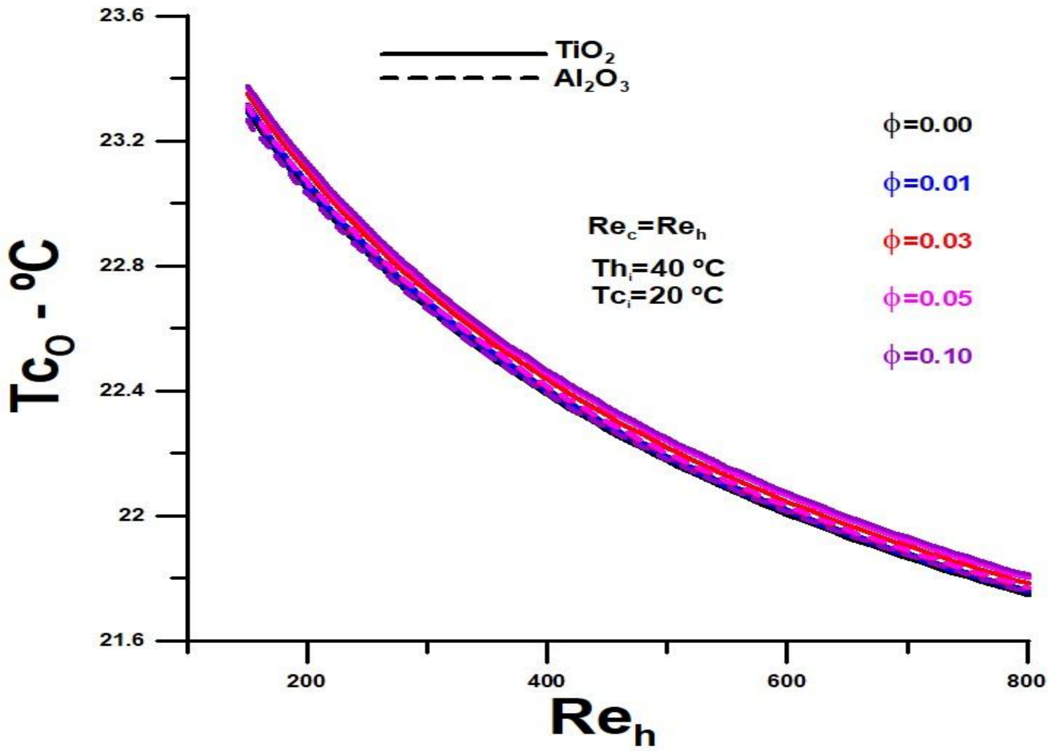

Figure 16 – Cold fluid temperature exit versus Reynolds number of the hot fluid with Re_c=Re_h

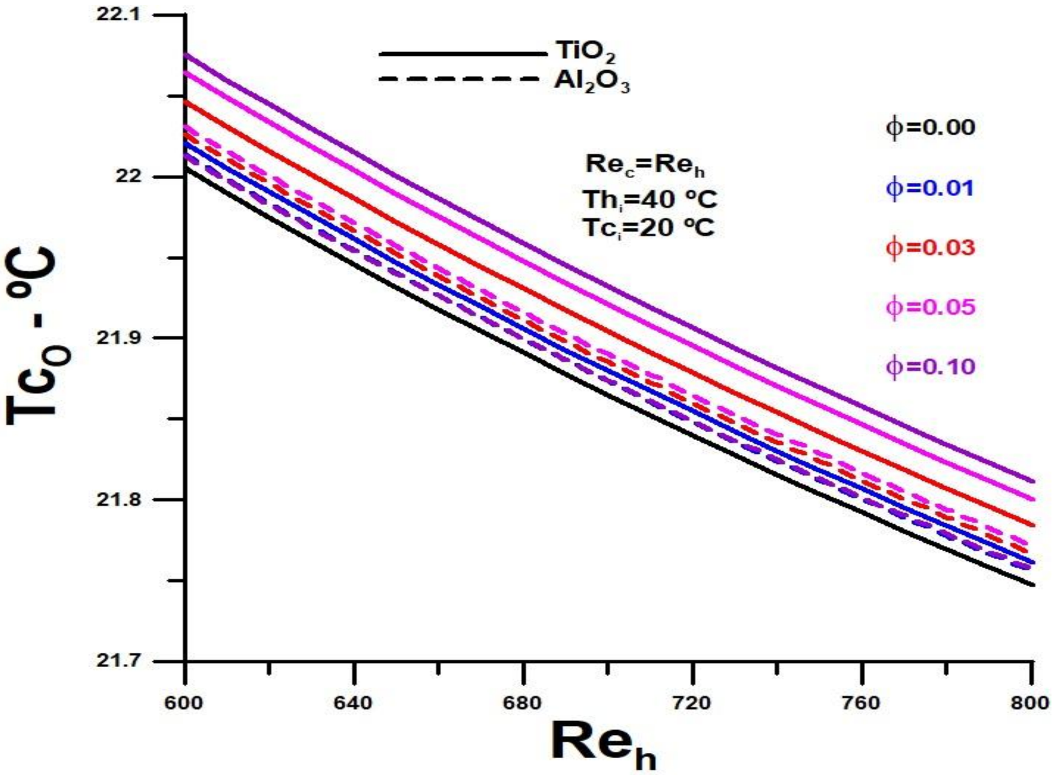

Figure 17 – Influence of the nanoparticles fraction at the cold fluid temperature exit for Re_c=Re_h

III. Conclusions

Through efficiency, effectiveness, irreversibility, and heat transfer rate, it is demonstrated that the thermal performance of the heat exchanger is strongly influenced by the flow rates in both fluids and the mass fraction of aluminum oxide nanoparticles (Al_2O_3) and titanium dioxide (TiO_2). In addition, aluminum oxide has a thermal performance slightly superior to titanium dioxide.

Thermal efficiency is high for the entire analyzed flow range, approaching 100% for high Reynolds numbers. Therefore, the nanoparticles do not present great relevance for determining the thermal efficiency within the analyzed volume fraction range. Furthermore, the influence of aluminum oxide is more noticeable than titanium dioxide.

Thermal effectiveness is reasonably high for low Reynolds numbers and average for higher Reynolds numbers. More significant fractions of nanoparticles have higher values for effectiveness.

Thermal irreversibility shows the same trend as effectiveness, decreasing with the Reynolds number in both fluids. Higher volume fractions of nanoparticles enable greater irreversibility, with greater weight for aluminum oxide.

For smaller Reynolds numbers, the closest is the actual heat transfer rate from the maximum possible heat transfer rate, which is reflected for high values of effectiveness and irreversibility. When the Reynolds numbers increase, the distance between the observed values for the actual heat transfer rate and the maximum heat transfer rate is further apart, implying lower values for effectiveness and irreversibility. The possibility of increasing the heat transfer rate between the fluids, which has a defined physical limit, decreases for high Reynolds numbers. However, there is a greater possibility of variation for the Reynolds number for the hot fluid since it has the minimum thermal capacity and determines the maximum heat transfer rate for the process under analysis. Besides this, when the Reynolds number of fluid increases, the difference between the local heat transfer rates decreases, tending towards zero.

Where there is greater irreversibility and greater energy exchange between the fluids, the hot fluid outlet temperature is lower. The hot fluid exit temperature is smaller for a low Reynolds number value in both fluids, and the cold fluid outlet temperature is more significant.

Finally, it can be stated that the influences of the mass flow rates of both fluids on the thermal performance of the heat exchanger are superior to the results obtained by the nanoparticles within the analyzed volume fraction range.

Reference

[1]. B. Zohuri (2017). "Compact Heat Exchanger Types and Application." Chapter 2, Springer International Publishing Switzerland. DOI 10.1007/978-3-319-29835-1_2

[2]. - Zafar Said and Rahman Saidur (2017). "Thermophysical Properties of Metal Oxides Nanofluids." Chapter 3, Nanofluid Heat and Mass Transfer in Engineering Problems, Intech Open. http://dx.doi.org/10.5772/65610

[3]. - Jang-Won Seo, Yoon-Ho Kim, Dongseon Kim, Young-Don Choi, and Kyu-Jung Lee (2015). "Heat Transfer and Pressure Drop Characteristics in Straight Microchannel of Printed Circuit Heat Exchangers." Entropy **2015**, *17*, 3438-3457. DOI:10.3390/e17053438

[4]. Emanuele Zanetti, Marco Azzolin, Stefano Bortolin, Giulio Busato, Davide Del Col (2018). "Design And Testing of a Microchannel Heat Exchanger Working As Condenser And Evaporator." International Refrigeration and Air Conditioning Conference. Paper 2033. https://docs.lib.purdue.edu/iracc/2033

[5]. Salah Almurtaji, Naser Ali, Joao A. Teixeira, Abdulmajid Addali (2020). "On the Role of Nanofluids in Thermal-Hydraulic Performance of Heat Exchangers—A Review." Nanomaterials 2020, 10, 734. DOI:10.3390/nano10040734

[6]. Yanhui Hana, Yan Liua, Ming Liaa, Jin Huanga (2012). "A review of development of micro-channel heat exchanger applied in air-conditioning system." Energy Procedia 14, 148-153. DOI:10.1016/j.egypro.2011.12.910

[7]. Harish Kumar Patel, RupeshKumar Khutey, Charles Xalxo (2015). "Preparation and application of nanofluid with microchannel and its experimental and theoretical thermal performance - A Review" IOSR Journal of Engineering (IOSRJEN), Vol. 05, Issue 04, (April. 2015), V3, PP 64-80.

[8]. Seungjoon Baik, Seong Gu Kim, Seongmin Son1, Hyeon Tae Kim, Jeong Ik Lee (2015). "Printed Circuit Heat Exchanger Design, Analysis and Experiment." NURETH-16, Chicago, IL, August 30-September 4.

[9]. Sushant S. Bhosale, Anil R. Acharya (2020). "Review On Applications of Micro Channel Heat Exchanger." International Research Journal of Engineering and Technology (IRJET), Volume: 07 Issue: 03.

[10]. Lei Chai, Savvas A. Tassou (2020). " A review of printed circuit heat exchangers for helium and supercritical CO2 Brayton cycles." Thermal Science and Engineering Progress, 18 (2020) 100543. https://doi.org/10.1016/j.tsep.2020.100543

[11]. Ahmad Fakheri (2007). "Heat Exchanger Efficiency." Transactions of the ASME, Vol. 129, pp. 1268- 1276. http://dx.doi.org/10.1016/j.applthermaleng.2017.05.076

[12]. Tiwari R, Maheshwari G (2017). "Effectiveness and efficiency analysis of parallel flow and counter flow heat exchangers." IJAIEM; 6:314-319.

[13]. Nogueira E. (2020). "Thermal performance in heat exchangers by the irreversibility, effectiveness, and efficiency concepts using nanofluids." Journal of Engineering Sciences, 7: F1-F7. DOI: 10.21272/jes.2020.7(2).f1.

[14]. Nogueira, E. (2021). "Efficiency and Effectiveness Thermal Analysis of the Shell and Helical Coil Tube Heat Exchanger Used in an Aqueous Solution of Ammonium Nitrate Solubility (ANSOL) with 20% H2O and 80% AN." Journal of Materials Science and Chemical Engineering, 2021, 9, 24-45. https://doi.org/10.4236/msce.2021.96003

Élcio Nogueira. "Second Law Applied to a Straight Microchannel Printed Circuit Heat Exchanger using TiO2 and Al2O3 as Nanoparticles." *IOSR Journal of Mechanical and Civil Engineering (IOSR-JMCE)*, 19(1), 2022, pp. 49-62.